arXiv:1405.7332v1 [astro-ph.HE] 28 May 2014



# Electron Heating, Magnetic Field Amplification, and Cosmic Ray Precursor Length at Supernova Remnant Shocks

J. Martin Laming[1], Una Hwang[2], Parviz Ghavamian[3] & Cara Rakowski[4]

## ABSTRACT

We investigate the observability, by direct and indirect means, of a shock precursor arising from magnetic field amplification by cosmic rays. We estimate the depth of such a precursor under conditions of nonresonant amplification, which can provide magnetic field strengths comparable to those inferred for supernova remnants. Magnetic field generation occurs as the streaming cosmic rays induce a plasma return current, and may be quenched either by nonresonant or resonant channels. In the case of nonresonant saturation, the cosmic rays become magnetized and amplification saturates at higher magnetic fields. The precursor can extend out to $10^{17} - 10^{18}$ cm and is potentially detectable. If resonant saturation occurs, the cosmic rays are scattered by turbulence and the precursor length will likely be much smaller.

The dependence of precursor length on shock velocity has implications for electron heating. In the case of resonant saturation, this dependence is similar to that in the more familiar resonantly generated shock precursor, which when expressed in terms of the cosmic ray diffusion coefficient $\varkappa$ and shock velocity $v_s$ is $\varkappa/v_s$. In the nonresonantly saturated case, the precursor length declines less

[1]Space Science Division, Naval Research Laboratory, Code 7684, Washington DC 20375
laming@nrl.navy.mil

[2]University of Maryland
Una.Hwang-1@nasa.gov

[3]Dept. of Physics, Astronomy and Geosciences, Towson University, Towson, MD 21252
pghavamian@towson.edu

[4]formerly of Naval Research Laboratory

quickly with increasing $v_s$. Where precursor length proportional to $1/v_s$ gives constant electron heating, this increased precursor length could be expected to lead to higher electron temperatures for nonresonant amplification. This should be expected at faster supernova remnant shocks than studied by previous works. Existing results and new data analysis of SN 1006 and Cas A suggest some observational support for this idea.

## 1. Introduction

Though diffusive shock acceleration has for many years been accepted as the theory of cosmic ray acceleration at shock waves, the associated cosmic ray precursor has never been convincingly detected in an astrophysical environment. The realization that cosmic rays in the preshock region may amplify magnetic field by resonant (Bell & Lucek 2001; Lucek & Bell 2000) or nonresonant (Bell 2004, 2005) instabilities, means that Alfvén Mach numbers and associated shock physics can be considerably different from the case without cosmic rays. These changes may offer a means of detecting or inferring the existence of such a precursor, either by direct imaging, or indirectly by the effects the precursor has on ambient plasma. Such plasma heating, produced by streaming cosmic rays, through their generation of plasma waves which are subsequently damped by the ambient medium, has been recently considered in other applications (e.g. Nekrasov & Shadmehri 2012; Stroman et al. 2012; Wiener et al. 2013). Magnetic field amplification by similar processes also considerably increases the rate of cosmic ray acceleration, possibly allowing supernova remnants to generate galactic cosmic rays up to the "knee" (around $10^{15}$ eV) and maybe beyond in the cosmic ray energy distribution.

In related work, the quasi-thermal electron heating at a number of supernova remnant shocks has been investigated observationally. In shocks capable of accelerating cosmic rays – so-called collisionless shocks where the shock transition occurs on a length scale much shorter than the ion mean free path against Coulomb collisions – the relative lack of collisions to enforce thermal equilibrium means that the electron and ion temperatures, $T_{e,i}$, are not necessarily equal. In general $T_i > T_e$ following from the shock jump conditions applied separately to electron and ion fluids. The temperature ratio, $T_e/T_i$ has been shown to follow an approximate law $T_e/T_i \propto 1/v_s^2$ law (where $v_s$ is the shock velocity Ghavamian et al. 2007a; van Adelsberg et al. 2008; Ghavamian et al. 2013), at least for those cases where neutral H exists upstream of the shock to give rise to H$\alpha$ emission at the shock front itself. Ghavamian et al. (2007a) suggested that such a behavior could arise if electrons are heated in a shock precursor established by the shock accelerated cosmic rays. Ths precursor extends a

length $\varkappa/v_s$, allowing heating for a time $\varkappa/v_s^2$, where $\varkappa$ is the cosmic ray diffusion coefficient, assumed independent of the shock velocity $v_s$. If the extent of the electron heating precursor is instead characterized by an ion gyroradius, $\sim v_s/\Omega$, where $\Omega$ is the appropriate cyclotron frequency (e.g. Cargill & Papadopoulos 1988), $T_e/T_i$ independent of shock velocity would be expected, contrary to observations. No specific scenario of cosmic ray acceleration or magnetic field amplification was discussed by Ghavamian et al. (2007a), though Rakowski et al. (2008) pointed out that the waves envisaged by Ghavamian et al. (2007a) are more efficiently excited at perpendicular shocks, and that such a geometry would naturally arise as a result of cosmic ray driven magnetic field amplification.

While magnetic field amplification is generally supported by Chandra observations of thin rims in X-ray synchrotron emission delineating the blast waves of SNRs, the level and mechanism of saturation remain controversial. Observational estimates by various authors at Cas A (Vink & Laming 2003), SN 1006 (Long et al. 2003; Yamazaki et al. 2004) and Tycho (Warren et al. 2005; Cassam-Chenaï et al. 2007) and other SNRs all summarized by Völk et al. (2005) generally reveal preshock magnetic fields in the range 100 - 500 $\mu$G, far greater than the typical ambient magnetic field. Such fields can be consistent with the expectations of Bell (2004, 2005), who suggested that the magnetic field amplifies through a nonresonant instability, driven by the cosmic ray current, which saturates at a higher magnetic field level than the resonant instability. As this nonresonant instability proceeds, cylindrical cavities oriented along the pre-existing magnetic field develop. Here the high energy (i.e. unmagnetized) cosmic rays reside, with the background plasma, and presumably the magnetized cosmic rays expelled into the interfaces between neighboring cavities (see e.g. Caprioli & Spitkovsky 2012). Resonant magnetic field amplification produces much lower field, with $\delta B \sim B$, and cannot explain such observations. Other authors (Luo & Melrose 2009) argue that nonresonant magnetic field amplification must inevitably produce turbulence, and that the pitch angle scattering of cosmic rays in this turbulence reduces their anisotropy and velocity relative to the upstream medium, quenching the magnetic field amplification without producing any macroscopic structures upstream. Features of this scenario, especially the isotropization of the cosmic rays, are reproduced in various kinetic simulations (Riquelme & Spitkovsky 2009; Stroman et al. 2009; Gargaté et al. 2010). This resonant saturation of the nonresonant instability also produces lower magnetic field than the nonresonant saturation envisaged by Bell (2004, 2005), and again, lower field than is generally observed.

Yet another alternative means of magnetic field amplification at shock waves, that of the interaction of the shock with pre-existing turbulence, is discussed by Giacalone & Jokipii (2007). Solenoidal motions induced by this interaction generate magnetic field as it moves with the fluid. In its simplest form, this mechanism does not produce a shock precursor, and

magnetic field is only amplified at the shock itself or just downstream from it, but can reach values as high as equipartition with the shocked plasma. Beresnyak et al. (2009) describe another version of such a model where the precursor in a cosmic ray modified shock interacts with turbulence and amplifies magnetic field upstream. Here the magnetic field amplification is driven by the cosmic ray pressure gradient, so the magnetic fields attained are lower than in Giacalone & Jokipii (2007), but still higher than the nonresonant instability of Bell (2004) and Bell (2005). Unlike the Giacalone & Jokipii (2007) model, Beresnyak et al. (2009) allow the cosmic ray acceleration rate to be increased by the magnetic field amplification, with the proviso that the initial cosmic ray acceleration and modification of the shock must occur with an undisturbed upstream medium. Drury & Downes (2012) revisit this and find somewhat lower magnetic field amplification, but still sufficient to match observational inferences.

In this paper, we investigate how far the inference that $T_e/T_i \propto 1/v_s^2$ may hold in conditions that cosmic rays nonresonantly amplify magnetic field, followed by either resonant or nonresonant saturation. In section 2 we estimate the characteristic length of the shock cosmic ray precursor under different conditions of magnetic field amplification and saturation, to compare with $L = \varkappa/v_s$ in the purely resonant case. In section 3, we collect these results and discuss how electron heating may vary with shock velocity and degree of magnetization of the preshock cosmic rays. Section 4 applies these ideas to observational results from the forward shocks of Cas A and SN 1006, and section 5 concludes. Details of assumptions concerning the cosmic ray distribution function are given in an appendix.

## 2. Magnetic Field Amplification

### 2.1. Introduction

As mentioned above, preshock magnetic field may be amplified by either resonant or nonresonant instabilities. Resonant amplification occurs when an individual cosmic ray gyrofrequency is Doppler shifted into resonance with a specific wave mode (Alfvén or fast mode, both commonly referred to as Alfvén waves when parallel propagating), and energy is transfered from particle to wave or vice versa occurs. This typically saturates when $\delta B \sim B$ or less, because at this stage the wave-particle resonance is lost and amplification ceases. Nonresonant magnetic field amplification is essentially an MHD process. The current associated with the drifting cosmic rays (or more properly the return current so induced in the background plasma) amplifies Alfvén waves, typically with $k_\parallel r_g >> 1$ (in the resonant case $k_\parallel r_g \sim 1$, where $k_\parallel$ is the parallel wavevector, and $r_g$ is the cosmic ray gyroradius). There is no individual wave-particle resonance. Bell (2004, 2005) has discussed nonlinear nonresonant saturation of this process, whereby unmagnetized cosmic rays and their associated magnetic

field expel the ambient plasma from cylindrical filaments, shutting down the return current as the plasma becomes magnetized. Other authors (e.g. Luo & Melrose 2009; Gargaté et al. 2010) have discussed a resonant means of saturating the nonresonant magnetic field growth, as the cosmic ray current is limited by pitch angle angle scattering in turbulence. In the following subsections we estimate the magnetic field amplification level and precursor distance over which this amplification occurs in both regimes of saturation.

### 2.2. Resonant Saturation of Nonresonantly Amplified Field by Cosmic Ray Pitch Angle Diffusion

Various kinetic simulations of nonresonantly amplified magnetic field (Riquelme & Spitkovsky 2009; Stroman et al. 2009; Gargaté et al. 2010) suggest that cosmic ray induced magnetic field saturates not according to the Bell (2004, 2005) scenario outlined above, but by the generation of turbulence that scatters the cosmic rays and reduces their drift relative to the upstream medium. We discuss here the level of magnetic field amplification and the length of the associated precursor to be expected in such a scenario.

We follow in part the analytical description of this saturation process given by Luo & Melrose (2009). The rate of change of the cosmic ray streaming speed ahead of the shock, $v_{CR} = \int f v_z d^3p$, where $f$ is the cosmic ray distribution function normalized to unity and $v_z$ the $z$-component of an individual cosmic ray velocity vector, due to scattering in turbulence is usually given as

$$\frac{dv_{CR}}{dt} = \int f \frac{dv_z}{dt} d^3p = - \int f \left\langle D \right\rangle v_z d^3p, \tag{1}$$

where $\left\langle D \right\rangle = \int_{-1}^{1} (1-\mu^2)\, D d\mu/2$ with $D = (\pi/4)\,(\Omega_{i0}/\left\langle \gamma \right\rangle)\,(\delta B^2/B^2)$, the cosmic ray pitch angle scattering diffusion coefficient. Here $\Omega_{i0}$ is the proton cyclotron frequency calculated with the initial magnetic field $B$, ($\Omega_i$ will be the same quantity calculated with the amplified field $\delta B$), $\left\langle \gamma \right\rangle$ is the average cosmic ray Lorentz factor, and $\delta B^2/B^2 << 1$ is assumed. We extrapolate this to the case of magnetic field amplification by the nonresonant instability, where $\delta B^2/B^2 << 1$ no longer holds, as follows. Since the nonresonant instability preferentially grows magnetic field with $kr_g >> 1$, only cosmic rays with pitch angle cosines $\mu \simeq \pm 1/kr_g$ interact with the turbulence. The limits on the integral over $\mu$ become $\pm 1/kr_g$ and $\left\langle D \right\rangle = (\pi/4)\,(\Omega_{i0}/\left\langle \gamma \right\rangle)\,(\delta B^2/B^2)\,/kr_g$. The particle scattering rate remains less than the gyrofrequency, even though $\delta B^2/B^2 >> 1$, due to the presence of the factor $kr_g$ in the denominator. Assuming $\delta B \propto \exp(\Gamma t)$, we can integrate equation 1. Luo & Melrose (2009) insert a growth rate $\Gamma = \sqrt{2} k_\parallel v_A \sqrt{4\pi J_{CR}/k_\parallel cB - 1} \simeq (6\eta k r_{g0})^{1/2} (v_s/c)^{3/2}\, \Omega_{CR}$ and derive $\delta B^2/B^2$ in the range 10-100. These values are lower than the nonresonant saturation, and

so saturation by resonant diffusion, suppressing the cosmic ray flow speed with respect to the upstream medium, will occur first if allowed.

The approximate expression for the growth rate above neglects the last term in the square root, and so overestimates the growth rate. This is not a very serious problem, except where the cosmic ray drift velocity is approaching the saturation value where $\Gamma \to 0$. We prefer to take $\Gamma = \sqrt{2} k_{\parallel max} v_A$, the maximum value of the growth rate at parallel wavevector $k_{\parallel max} = J_{CR} B / 2\rho c v_A^2 = 2\pi J_{CR} B / c \delta B^2$, which may both be rewritten with $\omega_{pi}$ and $\Omega_i$ as the upstream ion plasma and cyclotron frequencies respectively as

$$\Gamma = \frac{3\eta}{\sqrt{2}} \frac{\omega_{pi}}{\gamma_1 \gamma_{max}} \frac{\gamma_{max} - 3\gamma_1/4}{\ln \gamma_{max} - 1} \frac{v_s^2 v_{CR}}{c^3} \frac{B}{\delta B}$$
$$= 0.013 \frac{\eta \sqrt{n_i}}{\gamma_1 \gamma_{max}} \frac{\gamma_{max} - 3\gamma_1/4}{\ln \gamma_{max} - 1} \frac{B}{\delta B} \left( \frac{v_s}{5000 \text{ km s}^{-1}} \right)^2 \left( \frac{v_{CR}}{5000 \text{ km s}^{-1}} \right) \text{ s}^{-1} \quad (2)$$

and

$$k_{\parallel max} r_g = \frac{3\eta}{2} \frac{\omega_{pi}^2}{\Omega_i^2} \frac{v_s^2 v_{CR}}{c^3} \frac{\gamma_{max} - 3\gamma_1/4}{\ln \gamma_{max} - 1} \frac{\gamma}{\gamma_{max} \gamma_1}$$
$$= 15340 \eta n_i \left( \frac{v_s}{5000 \text{ km s}^{-1}} \right)^2 \left( \frac{v_{CR}}{5000 \text{ km s}^{-1}} \right) \left( \frac{3\mu\text{G}}{B} \right)^2 \left( \frac{B}{\delta B} \right)^2 \frac{\gamma_{max} - 3\gamma_1/4}{\ln \gamma_{max} - 1} \frac{\gamma}{\gamma_{max} \gamma_1} \quad (3)$$

Here, the current $J_{CR}$ is assumed to be carried by unmagnetized cosmic rays with Lorentz factors $\gamma_1 < \gamma < \gamma_{max}$, as given in the Appendix, with an additional flux coming from cosmic rays escaping the shock upstream at $\gamma \geq \gamma_{max}$, given by Bell et al. (2013) approximately as $n_{CR} v_s / 4\gamma_{max}$. The ratio of cosmic ray pressure to the shock ram pressure $\eta$ and $\gamma_1$ are assumed to be independent of $\delta B$. We substitute equation 3 into equation 1 and integrate the right hand side over $p$, assuming $f \propto 1/p^4$. In equation 1, we rewrite $dv_{CR}/dt \to v_{CR} dv_{CR}/dz$. With $\delta B / B \sim \exp(\Gamma z / v_{CR})$, we put $dv_{CR}/dz \simeq -v_{CR}/z \simeq \Gamma / \ln(\delta B / B)$ in equation 1 to find

$$\ln \left( \frac{\delta B}{B} \right) \frac{\delta B^5}{B^5} \simeq \frac{9\sqrt{2}}{\pi} \frac{\omega_{pi}^3}{\Omega_{i0}^3} \frac{v_s^6}{c^6} \eta^2 \left( \frac{\gamma_{max} - 3\gamma_1/4}{\ln \gamma_{max} - 1} \right)^2 \left( \frac{1 + \gamma_{max} \gamma_1}{\gamma_{max}^2 \gamma_1^2} \right)$$
$$= 8349 \left( \frac{v_s}{5000 \text{ km s}^{-1}} \right)^6 \left( \frac{3\mu\text{G}}{B} \right)^3 n_i^{3/2} \eta^2 \left( \frac{\gamma_{max} - 3\gamma_1/4}{\ln \gamma_{max} - 1} \right)^2 \left( \frac{1 + \gamma_{max} \gamma_1}{\gamma_{max}^2 \gamma_1^2} \right). \quad (4)$$

This evaluates to $\delta B / B \sim 14 \left( v_s / 5000 \text{ km s}^{-1} \right)^{6/5} \left( \gamma_{max} / 10^6 \right)^{1/5}$ for $\eta \sim 0.1$, $n_i \sim 1$, and $\gamma_1 = 1$, similarly to Luo & Melrose (2009), but with different dependencies of $\delta B / B$ on the shock velocity and other parameters. Comparing with Gargaté et al. (2010) for example, where $\gamma_{max} \sim 10^3$, plugging in numbers for their models B1, B2 or B3 yields $\delta B / B \sim 14$, comparable to their simulation results.

This degree of magnetic field amplification is smaller than that inferred in the observations cited above, though within uncertainties, once the magnetic field compression by the shock is taken into account, the lower end of the postshock magnetic fields given above approaching $\sim 100\mu$G might be accessible.

The length scale over which this precursor develops is given by

$$L = \frac{v_{CR}}{\Gamma} \ln\left(\frac{\delta B}{B}\right) = \frac{\sqrt{2}}{3}\frac{c^3}{v_s^2}\frac{\delta B}{B} \ln\left(\frac{\delta B}{B}\right) \frac{\gamma_1 \gamma_{max}}{\gamma_{max} - 3\gamma_1/4} \frac{(\ln \gamma_{max} - 1)}{\eta \omega_{pi}} \tag{5}$$

which evaluates to approximately $4\times10^{10} \left(5000 \text{ km s}^{-1}/v_s\right)^2 (\delta B/B) \ln(\delta B/B)\, \gamma_1 \ln \gamma_{max}/\eta\sqrt{n_i}$ cm for $\gamma_{max} >> \gamma_1$. With unmagnetized cosmic rays, $\gamma_1 \simeq 1$, and $L \sim 10^{12} \left(5000 \text{ km s}^{-1}/v_s\right)^2 \ln \gamma_{max}/\eta$ cm. The precursor to the shock in model B2 of Gargaté et al. (2010) is thus predicted to be $8\times10^{12}$ cm deep, in good agreement with the simulated value $(v_s/\Gamma_{max}) \ln(\delta B/B) \simeq 4\times10^{12}$ cm. Where $\delta B/B$ is approximately proportional to $v_s^{6/5}$, $L \propto v_s^{-4/5} \ln v_s$ which is close to the $L \propto 1/v_s$ discussed above. Calculating $r_g$ with $\delta B$ rather than $B$ in equation 3 would give $\delta B/B \propto v_s$ and $L \propto v_s^{-1} \ln v_s$, even closer to the behavior seen in the data. We emphasize that $L$ represents the cosmic ray precursor associated with magnetic field amplification, and is of course much smaller than the cosmic ray precursor associated with resonant wave generation and scattering, given approximately by $\langle D \rangle / v_s$.

If the unmagnetized cosmic ray spectrum extends down to nonrelativistic energies so that $\gamma_1 \sim 1$, then this precursor is predicted to be too small to be spatially resolvable, $\sim 10^{14}$ cm for $\eta \sim 0.1$ and $n_i \sim 1$. Significant magnetization of cosmic rays, increasing $\gamma_1$, lengthens the precursor, but also reduces the eventual magnetic field so long as resonant saturation remains effective. Such magnetization though is more likely in the case of nonresonant saturation discussed below, where higher magnetic fields can result.

### 2.3. Nonresonant Saturation

Bell (2005) argues that cosmic ray induced magnetic field amplification should saturate as the unmagnetized cosmic rays and their associated magnetic field expel the ambient plasma from cylindrical filaments.

We can examine the expected magnitude of the amplified field at saturation by considering the nonresonant instability (Bell 2004, 2005). At saturation, $1/r_g < k_\parallel < J_{CR}B/n_i m_i c v_A^2 = 4\pi \left(n'_{CR} + n_{CR}/4\gamma_{max}\right) q v_s B/c\delta B^2$ where $n'_{CR}$ is the number density of unmagnetized cosmic rays with gyroradius $> r_g$. Consequently,

$$\delta B < \sqrt{4\pi n'_{CR} v_s m_i c \langle \gamma' \rangle}$$

$$< \sqrt{12\pi\eta n_i m_i v_s^3/c}\sqrt{\frac{\ln\gamma_{max} - \ln\gamma_1 + 1/4}{\ln\gamma_{max} - 1}}$$

$$< 5\times10^{-4}\sqrt{\eta n_i}\left(v_s/5000\text{ km s}^{-1}\right)^{3/2}\sqrt{\frac{\ln\gamma_{max} - \ln\gamma_1 + 1/4}{\ln\gamma_{max} - 1}}\text{G}. \quad (6)$$

This represents an amplification over the initial field, assumed to be $3\mu$G, of a factor of 10 - 50 (taking $\eta \sim 0.1$, $n_i \sim 1$ cm$^{-3}$), depending on the value assumed for the maximum Lorentz factor of magnetized cosmic rays, $\gamma_1$. This is about an order of magnitude higher than magnetic field amplification limited by resonant scattering.

We also calculate the magnetic precursor depth in the case that the growth is nonresonantly saturated, according to Bell (2004, 2005). We assume $\mathbf{k}\|\mathbf{B}$, as seen for example, even at oblique shocks, in simulations (Gargaté & Spitkovsky 2012) and in *in situ* observations (Bamert et al. 2004). Starting from Bell's expression for the growth rate we write the time evolution of the amplified magnetic field $\delta B$

$$\frac{d\delta B}{dt} = \sqrt{\frac{J_{CR}Bk}{\rho c} - k^2 v_A^2}\delta B = \sqrt{\frac{J_{CR}Bk}{\rho c} - \frac{k^2\delta B^2}{4\pi\rho}}\delta B. \quad (7)$$

We integrate to find the time $t$ over which this magnetic field develops

$$t = \int_B^{\delta B}\sqrt{\frac{\rho c}{J_{CR}Bk}}\frac{1}{\sqrt{1 - \frac{kc}{4\pi J_{CR}B}\delta B^2}}\frac{d\delta B}{\delta B}. \quad (8)$$

We then put $\delta B = \sqrt{4\pi J_{CR}B/kc}\cos\theta$ to write

$$t = -\sqrt{\frac{\rho c}{J_{CR}Bk}}\int_{\arccos\sqrt{kcB/4\pi J_{CR}}}^{\arccos\sqrt{kc\delta B^2/4\pi J_{CR}B}}\sec\theta d\theta = \sqrt{\frac{\rho c}{J_{CR}Bk}}\left[\ln\left|\tan\theta + \sec\theta\right|\right]_{\arccos\sqrt{kcB/4\pi J_{CR}}}^{\arccos\sqrt{kc\delta B^2/4\pi J_{CR}B}}. \quad (9)$$

Evaluating,

$$t = \sqrt{\frac{\rho c}{J_{CR}Bk}}\left[\ln\left|\frac{\sqrt{1-kcB/4\pi J_{CR}}}{\sqrt{kcB/4\pi J_{CR}}} + \sqrt{4\pi J_{CR}/kcB}\right| - \ln\sqrt{4\pi J_{CR}B/kc\delta B^2}\right]$$
$$= \sqrt{\frac{\rho c}{J_{CR}Bk}}\ln\left|\frac{\delta B}{B}\sqrt{1 - kcB/4\pi J_{CR}} + \frac{\delta B}{B}\right|. \quad (10)$$

At saturation, where $k = 4\pi J_{CR}B/c\delta B^2$, with $\delta B >> B$

$$t = \sqrt{\frac{n_i m_i}{4\pi}}\frac{\delta B}{B}\frac{c}{n'_{CR}qv_{CR} + n_{CR}qv_s/4\gamma_{max}}\ln\left(2\frac{\delta B}{B}\right) \simeq \frac{c^3\gamma_1\gamma_{max}}{3\eta v_s^2 v_{CR}\omega_{pi}}\frac{\ln\gamma_{max} - 1}{\gamma_{max} - 3\gamma_1/4}\frac{\delta B}{B}\ln\left(2\frac{\delta B}{B}\right). \quad (11)$$

The precursor depth is then

$$L = \frac{c^3}{3\eta v_s v_{CR} \omega_{pi}} \frac{\gamma_1 \gamma_{max}}{\gamma_{max} - 3\gamma_1/4} (\ln \gamma_{max} - 1) \frac{\delta B}{B} \ln \left( 2 \frac{\delta B}{B} \right) \quad (12)$$

This is similar in expression to the case of resonant saturation of the nonresonant instability. There is a missing factor of $\sqrt{2}$ in the numerical constant, and here $\delta B \propto v_s^{3/2}$. Also, for nonresonant saturation, $\gamma_1$ is likely to be significantly larger, yielding a longer cosmic ray magnetic field amplification precursor, as well as a higher magnetic field than in resonant saturation. Bell et al. (2013) argue that $\gamma_1 \sim \gamma_{max}$, in which case $L \sim 10^{13} \gamma_{max} \ln \gamma_{max} / \eta \sqrt{n_i}$ cm.

We can estimate the physical size of the precursor by taking $\gamma_{max} \sim 10^5$ (e.g. Bell et al. 2013; Vink & Laming 2003), to find $L \sim 10^{17} - 10^{18}$ cm, which is potentially resolvable by e.g. the 0.5 arcsecond angular resolution of Chandra for relatively nearby galactic supernova remnants. Morlino et al. (2010) and Winkler et al. (2014) consider the case of SN 1006 specifically. The different dependence of $\delta B$ on $v_s$ in this saturation case leads to $L \propto v_s^{-1/2} \ln v_s$, assuming $\gamma_1$ and $\gamma_{max}$ are independent of $v_s$. This is further from the $L \propto 1/v_s$ that produces the constant electron heating with shock velocity, and suggests that one should look at supernova remnants possibly subject to the Bell magnetic field amplification to see if evidence can be found for enhanced postshock electron temperatures because the magnetic precursor length decreases less quickly with increasing shock speed.

Another means of nonresonant saturation is discussed by Niemiec et al. (2010), following Winske & Leroy (1984). The background plasma can be accelerated by the nonresonant mode, gradually shutting down the cosmic ray current with respect to it. The principal requirement for this is a cold cosmic ray "beam", where the perpendicular temperature is much lower than the parallel temperature, and when the beam is cold, filamentation does not occur. Niemiec et al. (2010) argue that such a case may occur ahead of relativistic shocks, where only cosmic rays focussed along the shock velocity vector are able to outrun the shock and contribute to magnetic field amplification. The application to lower velocity SNR shocks appears less clear.

### 2.4. Resonant or Nonresonant Saturation?

Clearly, resonant saturation, if allowed, will restrict magnetic field amplification to only a factor of a few over the preshock ambient field. However observations of SNRs generally reveal much larger magnetic field amplification that this, suggesting that resonant saturation does not occur. Either nonresonant magnetic field amplification proceeds until nonresonant saturation sets in, or some other mechanism of magnetic field amplification is at work.

Assuming that nonresonant field amplification is at work, what should determine whether resonant or nonresonant saturation will occur? We argue that when the parallel wavevector of the amplification satisfies the inequality

$$\frac{1}{r_g} < k_\parallel < \frac{J_{CR}B}{\rho c v_A^2} = \frac{\gamma n_{CR}}{n_i}\frac{v_s^2}{v_A^2}\frac{\Omega_{CR0}}{v_s} < \frac{\Omega_{CR0}}{v_s}\frac{\delta B}{B} \tag{13}$$

resonant scattering should begin to be inhibited. This is because when $k_\parallel < \Omega_{CR}/v_s = (\Omega_{CR0}/v_s)\,(\delta B/B)$ at a parallel shock, the minimum drift velocity cosmic rays need to outrun the shock and form the precursor also moves them out of resonance with parallel propagating waves.[1] Substituting for $\delta B/B$ from equations 4 or 6 we get $v_s$ in the range

$$\left(\frac{v_s}{5000\text{km s}^{-1}}\right) < 0.21\left(\frac{B}{3\mu\text{G}}\right)^{-13/14} n_i^{-1/4}\eta^{-3/14}\left(\frac{\ln\gamma_{max}-1}{\ln\gamma_{max}-\ln\gamma_1+1/4}\right)^{5/14}$$
$$\rightarrow 0.64\left(\frac{B}{3\mu\text{G}}\right)^{-6/5} n_i^{-1/5}\eta^{-1/5}\left(\frac{\ln\gamma_{max}-1}{\ln\gamma_{max}-\ln\gamma_1+1/4}\right)^{1/5}, \tag{14}$$

respectively. To satisfy the conditions discussed by Bell (2004, 2005), we take $\gamma_1 \rightarrow \gamma_{max}$, $\eta \sim 0.1$, and the upper limit on $\delta B$ derived from equation 6. The equation 14 shows that resonant saturation is inhibited when $v_s <\sim 10,000$ km s$^{-1}$ (dropping the explicit dependencies on other parameters).

In considering the competition between resonant and nonresonant magnetic field amplification, Marcowith & Casse (2010) argue for a gradual transition between the two mechanisms over an order of magnitude in shock velocity, at similar values to those in equation 14, with resonant amplification dominating at lower shock velocities, since at saturation $\delta B \propto v_s$, whereas for nonresonant amplification $\delta B \propto v_s^{3/2}$. Conversely, we have just shown that resonant saturation is favored over nonresonant saturation at higher shock velocities, although this depends on assumptions about the dependence of $\eta$ on $v_s$.

The arguments we have made above also tacitly assume a parallel shock geometry. Bell (2005) gives the angular dependence of the nonresonant growth rate, $\Gamma$. Keeping $\mathbf{k}\|\mathbf{B}$,

$$x^3 + x^2\left[2+\beta\right] + x\left[1+2\beta-\frac{B^2j^2}{k^2v_A^4\rho^2}\right] + \beta - \frac{B^2j^2}{k^2v_A^4\rho^2}\left[(\beta-1)\cos^2\theta+1\right] = 0 \tag{15}$$

where $x = \Gamma^2/k^2v_A^2$, $\beta = c_s^2/v_A^2$, and $\theta$ is the angle between $\mathbf{k}$ and $\mathbf{j}$. At $\beta = 1$, the explicit angular dependence disappears and $\Gamma = kv_A\sqrt{Bj/k\rho v_A^2 - 1}$. Putting $k = k_{\parallel max}$ from

[1] At an oblique shock, the condition would be $k_\parallel \cos\theta_{bn} < \Omega_{CR}/v_s$ where $\theta_{bn}$ is the shock obliquity, and the waves are assumed still parallel propagating.

equation 3, $Bj/k_{\parallel max}\rho v_A^2 = 2$ and $\Gamma = k_{\parallel max} v_A$. For $0 \leq \beta \leq 1$, $k_{\parallel max} v_A \leq \Gamma \leq 1.25 k_{\parallel max} v_A$. We emphasize "explicit" angular dependence above, because $k_{\parallel max}$ may depend on shock obliquity through its proportionality to $\eta = (\ln \gamma_{max} - 1)\, c^2 n_{CR}/3 n_i v_s^2$. The variation of cosmic ray pressure $\eta$ with shock obliquity is very uncertain. The threshold energy for injection into the diffusive shock acceleration process increases with increasing obliquity (e.g. Zank et al. 2006), reducing the cosmic ray number density, but the acceleration rate in such geometry increases. The generation of turbulence however is much more likely to decrease with increasing obliquity (e.g. Laming et al. 2013), as does the cosmic ray current. These both make it likely that resonant scattering and saturation are even more inhibited in favor of nonresonant saturation in these cases of oblique shocks. Simply reinstating the obliquity in equation 13 leads to $v_s$ gaining an extra factor $\cos^{-5/14}\theta_{bn} \rightarrow \cos^{-2/5}\theta_{bn}$ in equation 14.

In cases where cosmic ray acceleration is efficient Reville & Bell (2013) show that amplified magnetic fields become highly disorganized, and essentially isotropic. The initial shock obliquity has little affect on the final magnetic field. This might support some of our arguments about the transition to turbulence above, but by assuming that the cosmic ray acceleration is "efficient", Reville & Bell (2013) avoid the shock injection issue. Caprioli & Spitkovsky (2012) show that nonresonant saturation is still obtained at shock obliquities of 20°, using large scale hybrid simulations, but they comment that the effect is particularly evident at parallel shocks. This implication is contrary to our speculation above.

In summary, whether nonresonant magnetic field amplification saturates resonantly or nonresonantly depends on the value of $\eta$ and its dependence on $v_s$, and remains unclear. Much of this uncertainty can be traced to the problem of particle injection into diffusive shock acceleration, and so appears unlikely to have a simple solution. However one clear difference between these two regimes appears to be in the extent of the cosmic ray induced magnetic field shock precursor to be expected. This is something that could be possibly exploited observationally to identify the saturation mechanism and we return to discuss it further below.

### 2.5. Rakowski, Laming & Ghavamian (2008) Revisited

Following the inference of Ghavamian et al. (2007a) that electrons at collisionless shocks may be heated in the cosmic ray precursor, Rakowski et al. (2008) estimated the growth rate of lower hybrid waves in the cosmic ray amplified magnetic field. Lower hybrid waves are electrostatic ion oscillations directed almost perpendicularly to the magnetic field in conditions where the electrons are magnetized (electron gyroradius << wavelength), inhibiting

the electron screening of the oscillation that would otherwise occur. The wave phase velocity perpendicular to the magnetic field is much smaller than that along it, allowing the wave to simultaneously be in resonance with unmagnetized ions and magnetized electrons.

Rakowski et al. (2008) calculated a kinetic growth rate of lower hybrid waves in a cosmic ray precursor, showing that the reactive growth for plausible cosmic ray distribution functions is zero. We correct here a small error in the final step of their calculation. We give a revised version of their equation 5 for the growth rate of lower hybrid waves in a cosmic ray precursor, where the cosmic rays are assumed to be in a "kappa"-distribution with index $\kappa$, where $\kappa = 2$ corresponds to the $p^{-4}$ spectrum familiar in first order Fermi acceleration,

$$\gamma = \left(\frac{\pi}{\kappa}\right)^{3/2} \frac{q^2}{p_t k} \frac{\omega^3 n_{CR}}{\omega_{pi}^2 + \omega_{pe}^2 \cos^2\theta} \frac{(2\kappa-3)\Gamma(\kappa)}{\sqrt{2}\Gamma(\kappa-1/2)} \int \delta(\omega - \mathbf{k}\cdot\mathbf{v})$$
$$\times \left\{ -\left[1 + \frac{(p_x - mv_s)^2}{2\kappa p_t^2}\right]^{-\kappa} \frac{(p_x - mv_s)}{p_t^2} \frac{k}{|k|} + \frac{\kappa}{\kappa-1} \frac{xv_s}{\varkappa^2} \frac{\partial \varkappa}{\partial p_x} \left[1 + \frac{(p_x - mv_s)^2}{2\kappa p_t^2}\right]^{1-\kappa} \right\}$$
$$\times e^{-xv_s/D} dp_x. \tag{16}$$

This is modified from the original version by the factor $k/|k|$ multiplying the first term in curly brackets. This arises from the scalar product $\mathbf{k}\cdot\partial f/\partial\mathbf{p}$, and restricts the region of $p_x$ where the growth rate may be positive to $0 < p_x < mv_s$. When the momentum dependence of $\varkappa$ is neglected, maximum growth is found at $p_x = 0.7mv_s$ for $\kappa = 2$ with rate

$$\gamma_1 = 0.04 \frac{n_{CR}}{n_i} \omega. \tag{17}$$

It is not possible in this case for lower hybrid waves to stay in contact with the shock, as in Laming (2001a) and Laming (2001b), but in the context of an extended cosmic ray precursor (as opposed to a narrow precursor due to shock reflected ions extending about one gyroradius upstream), this does not greatly affect their growth. If the second term involving $\partial\varkappa/\partial p_x$ dominates the growth rate, maximum growth is found at $p_x = \pm\sqrt{13}mv_s/2$, also for $\kappa = 2$, with rate

$$\gamma_2 = 0.17 r \frac{n_{CR}}{n_i} \omega, \tag{18}$$

where the cosmic ray diffusion coefficient $\varkappa \propto p^r$. At a parallel shock $r = 1/3 - 1/2$ for Kolmogorov or Kraichnan turbulence respectively, whereas $r = 1/9 - 1/6$ at a perpendicular shock (see Appendix A in Rakowski et al. 2008). Thus the two terms are likely to contribute a similar order of magnitude to the growth rate. This is a factor of about 2 smaller than that originally given ($\gamma = 0.14\,(n_{CR}/n_i)\,\omega$) in the most appropriate case of a perpendicular shock. Rakowski et al. (2008) compared the growth rate for lower hybrid waves with that for magnetic field amplification, assuming that the same cosmic rays are responsible for

both. They thus determine a critical Alfvén Mach number (of order 10) where magnetic field amplification ceases and lower hybrid wave generation takes over. This argument is most appropriate for resonant saturation, where the magnetization of cosmic rays is not effective in saturating the growth. To explain other cases, the growth rate of Rakowski et al. (2008) needs to be modified to include only the unmagnetized cosmic rays.

### 2.6. Saturation of Magnetic Field Amplification by Electron Heating?

To examine the effect of electron heating, we compare the growth rates for magnetic field amplification and lower hybrid waves. At full nonresonant saturation, the unmagnetized cosmic rays and ambient plasma do not overlap, and the growth of lower hybrid waves should be suppressed. In such a case, the treatment of Rakowski et al. (2008) may become invalid. However it is important to be aware that the inference $T_e/T_i \propto 1/v_s^2$ is determined from SNR shocks that have neutral material in their preshock media, and generally do not show strong X-ray synchrotron emission. As such these are unlikely to be the strongest cosmic ray acceleration sites, and presumably have not saturated their magnetic field amplification in this manner. It is even possible that the electron heating itself prevents the magnetic field amplification from saturating.

We compare the growth rate for waves that heat electrons, $\Gamma \simeq 0.07\omega n_{CR}/n_i$ with the growth rate for magnetic field amplification, $\Gamma = \sqrt{2}k_{\parallel max}v_A$. We find

$$\frac{\delta B^2}{B^2} = \frac{\omega_{pi}}{\Omega_{i0}}\sqrt{\frac{m_e}{2m_i}}\frac{v_{CR}}{c}\frac{1}{0.07} \simeq 180\left(\frac{v_s}{5000\mathrm{km\ s^{-1}}}\right)\sqrt{n_i}\left(\frac{3\mu G}{B}\right)\left(\frac{\gamma_{max}-3\gamma_1/4}{\gamma_{max}-\gamma_1}\right) \qquad (19)$$

The predicted amplified magnetic field is higher than that coming from nonresonant amplification saturated by resonant scattering, and so that result is unlikely to change. But in this case the magnetic field never grows to the level where lower hybrid wave growth competes with magnetic field amplification, so we do not expect significant electron heating when resonant saturation is important. However the field in equation 19 is *lower* than that expected from nonresonant saturation, and so the electron heating in a cosmic ray precursor might prevent the full nonlinear stage of that instability from developing, and electron heating by lower hybrid waves to take over from magnetic field amplification in dissipating the free energy of the cosmic ray current. From equation 12, we would also expect it to reduce the depth of the magnetic field shock precursor by a similar factor, i.e. about one order of magnitude.

The level of magnetic field saturation imposed by electron heating on the amplification by pre-existing turbulence is harder to assess. In the case that the magnetic field is amplified

by the shock itself (Giacalone & Jokipii 2007), the electron heating should have no effect. In the case discussed by Beresnyak et al. (2009) and Drury & Downes (2012), corresponding to the interaction of the cosmic ray precursor with pre-shock turbulence, the growth rate is approximately given by the vorticity resulting in the preshock flow following deceleration by the cosmic ray pressure gradient. This is $\Gamma \sim v_s \eta \delta\rho/\rho\lambda$, where $\delta\rho/\rho$ expresses the amplitude of the preshock turbulence, and $\lambda$ is the length scale over which the density varies. Equating this to the growth rate for lower-hybrid waves yields $\delta B \sim 2 \times 10^7 \, (\ln \gamma_{max} - 1) \, \delta\rho/\rho\lambda$ G. Specializing to the forward shock of Cas A, where $\lambda \sim 10^{18}$ cm and $\delta\rho/\rho \sim 10^3$, $\delta B \sim 2 \times 10^{-8} \, (\ln \gamma_{max} - 1)$ G. This is much lower than the observed field of order $10^{-4}$G, suggesting that such instabilities are not operating. Values of $\lambda$ as low as $10^{15}$ cm would be required. As Beresnyak et al. (2009) comment, the reason such instabilities may compete with the nonresonant current driven instability is that although the growth rate is intrinsically weaker, all the cosmic rays participate in the former. In the latter, only the very highest energy cosmic rays contribute. But because the growth rate is intrinsically weaker, the Beresnyak et al. (2009) instability is more easily saturated by electron heating.

## 3. Electron Heating

### 3.1. Electron Heating by Cosmic Rays and the Shock Velocity

We briefly recap. Ghavamian et al. (2007a) and van Adelsberg et al. (2008) report a dependence of electron temperature to ion temperature, $T_e/T_i$ immediately postshock approximately proportional to $1/v_s^2$ for a selection of supernova remnants exhibiting H$\alpha$ emission. If $T_i \propto v_s^2$, then $T_e$ is constant. Ghavamian et al. (2007a) put forward an explanation that electron heating in a cosmic ray precursor of length $L \sim \varkappa/v_s$, where $\varkappa$ is the cosmic ray diffusion coefficient would lead to such a dependence. The time spent in the precursor by preshock gas is then $t \sim \varkappa/v_s^2$, leading to electron heating $E = 0.5 m v_e^2 = 0.5 m D_{|||} t$ independent of $v_s$ if the electron velocity diffusion coefficient, $D_{|||}$, in waves excited in the precursor, is proportional to $v_s^2$. In the specific case of lower-hybrid waves considered by Ghavamian et al. (2007a), this is the case. In this discussion, no reference was made to the specific form of the cosmic ray precursor, but the required dependence $\varkappa \propto 1/B$ suggests a Bohm-like diffusion coefficient and magnetic field amplification via the resonant instability.

This far, it has been the purpose of this paper to investigate how far such behavior should persist into the regime of nonresonant magnetic field amplification. Rakowski et al. (2008) invoked magnetic field amplification as a means of ensuring a locally quasi-perpendicular shock (necessary for the generation of lower hybrid waves), and showed that at high Alfvén Mach number, magnetic field amplification has the higher growth rate, while at lower $M_A$ the

cosmic ray generation of lower hybrid waves wins. They estimated a critical $M_A \sim 6v_{inj}/v_s$ which would become $M_A \sim 3v_{inj}/v_s \sim 30$ with the correction to the lower-hybrid wave growth rate discussed above in equation 18, where $v_{inj} \sim 10v_s$ at a perpendicular shock is the injection velocity for diffusive shock acceleration. This is very similar to the estimate above in equation 19. In both of these (resonant and nonresonant) cases, the magnetic field amplification and lower hybrid wave generation is dependent on the streaming velocity of unmagnetized cosmic rays through the upstream medium.

Figure 1 illustrates schematically how we envisage the electron heating to vary with shock velocity. At relatively low shock velocities, where the cosmic rays amplify magnetic field by resonant interactions, $T_e$ is constant, according to the arguments above. At higher shock velocities, where nonresonant amplification can occur, $T_e$ can increase with shock velocity, as the precursor lengths over which magnetic field amplification can occur become larger (equations 5 and 12 for resonant and nonresonant saturation respectively). The curve for resonant saturation of the nonresonant instability is shown as a dotted line, because in this case magnetic field amplification probably always dominates and quenches the electron heating.

By way of contrast, Matsukiyo (2010) describes a calculation of instabilities excited by shock reflected ions at perpendicular shocks, which at low $M_A < 10$ predicts $T_e$ approximately independent of shock velocity, and increasing as $v_s^2$ at higher $M_A$. This arises because at low $M_A$, the modified two stream instability grows fastest, generating lower hybrid waves, and is driven to saturation where the electron gyroradius equals the electron inertial length, $v_{T_e}/\Omega_e \sim c/\omega_{pe}$, giving $n_e k_{\rm B} T_e \sim B^2/8\pi$. Thus so long as $B^2/n_e$ is constant, shocks of different velocity heat electrons to the same $T_e$. At higher $M_A$, the Buneman instability with faster growth rate takes over, leading to the sequence of growing Langmuir waves, heating electrons and then ion acoustic waves taking over, as modeled by Cargill & Papadopoulos (1988), leading to $T_e \propto v_s^2$.

### 3.2. Effect of Magnetized Cosmic Rays

We have argued that the shock velocity dependence of the length of shock precursors due to cosmic ray magnetic field amplification means that higher electron heating should be expected at shocks where nonresonant magnetic field amplification is dominant over resonant processes. Following Riquelme & Spitkovsky (2010), another possibility for electron heating at shocks undergoing nonresonant magnetic field amplification may exist, involving a drift instability of magnetized cosmic rays.

As cosmic rays streaming ahead of a shock amplify magnetic field, more and more cosmic rays at the lower end of the energy spectrum become magnetized. Their gyroradii in the stronger field are too small to allow them to stream ahead and contribute to the current that amplifies the field. Thus, according to the inequality 15, a shock with strong cosmic ray current that saturates resonantly may transition to nonresonant saturation (and higher magnetic field) if sufficient cosmic rays become magnetized to reduce $\gamma n_{CR}$ and hence satisfy the inequality. The resonant saturation of nonresonantly generated field occurs because streaming cosmic rays are scattered and isotropized by the turbulence. In this case, no electron heating by cosmic rays should occur, because the streaming motion is inhibited. Riquelme & Spitkovsky (2010) discuss an interesting exception to this rule. A drift current associated with magnetized cosmic rays may also amplify magnetic field. We argue below that it might also generate lower-hybrid waves and heat electrons.

Riquelme & Spitkovsky (2010) give a theory of the Perpendicular Current Driven Instability. In the presence of cross-$B$ density gradients, a cosmic ray drift current may develop along the vector $\nabla f_{CR} \times \mathbf{B}$. Riquelme & Spitkovsky (2010) estimate the cosmic ray drift velocity to be $\sim c/2$, so other instabilities besides the magnetic field amplification that they discuss could operate, including the generation of waves (e.g. lower hybrid waves) that could heat electrons.

Therefore, we briefly investigate a reactive instability driven by cosmic ray drift. In perpendicular propagation, the longitudinal part of the cold plasma dielectric tensor is

$$K^L = 1 + \frac{\omega_{pe}^2}{\Omega_e^2} + \frac{\omega_{pi}^2}{\Omega_i^2 - \omega^2} + \frac{\omega_{pCR}^2}{\Omega_{CR}^2 - \omega^2}\frac{\omega - \mathbf{k}\cdot\mathbf{v}_d}{\omega} = 0, \tag{20}$$

where $\omega_{pCR}$ and $\Omega_{CR}$ are the cosmic ray plasma and cyclotron frequencies respectively, and $\mathbf{v}_d$ is the cosmic ray drift velocity. We have assumed $\omega << \Omega_e$, the electron gyrofrequency. The dispersion relation is

$$\omega^5 - \omega^3\Omega_{LH}^2 + \omega^2\mathbf{k}\cdot\mathbf{v}_d\frac{n_{CR}}{\langle\gamma\rangle n_i}\Omega_{LH}^2 + \omega\Omega_{LH}^2\Omega_{CR}^2 - \mathbf{k}\cdot\mathbf{v}_d\frac{n_{CR}}{\langle\gamma\rangle n_i}\Omega_{LH}^2\Omega_i^2 = 0 \tag{21}$$

where $\Omega_{LH}^2 = \Omega_i\Omega_e$. As $\mathbf{k}\cdot\mathbf{v}_d \to 0$, the solutions are

$$\omega = 0, \quad \omega^2 = \frac{\Omega_{LH}^2}{2} \pm \frac{1}{2}\sqrt{\Omega_{LH}^4 - 4\Omega_{LH}^2\Omega_{CR}^2} \simeq \Omega_{LH}^2 \text{ or } \Omega_{CR}^2. \tag{22}$$

Reinstating the cosmic ray drift current, we find growing solutions at $\omega = \pm\Omega_{LH}$ when $\mathbf{k}\cdot\mathbf{v}_d n_{CR}/\langle\gamma\rangle n_i > 0.39\Omega_{LH}$. With $n_{CR}/\langle\gamma\rangle n_i \simeq 3\eta v_s^2/\langle\gamma\rangle^2 c^2$, $k \simeq \Omega_{LH}/v_i$ where $v_i \sim 10^6$ cm s$^{-1}$ is the ion thermal speed in the precursor, $v_d \simeq c/2$, we find $v_s^2 > 0.26 c v_i \langle\gamma\rangle^2/\eta$, or $v_s > 2.8\times10^8\langle\gamma\rangle$ cm s$^{-1}$, assuming $\eta \simeq 0.1$. So depending on the value of $\langle\gamma\rangle$ assumed,

one might expect to see a contribution to electron heating from magnetized cosmic rays start to become effective at shock velocities of order a few thousand km s$^{-1}$, which should exhibit itself as a break from the $T_e/T_i \propto 1/v_s^2$ law reported by Ghavamian et al. (2007a) and van Adelsberg et al. (2008). Such a contribution also has to compete with magnetic field amplification by magnetized cosmic rays, which has growth rate (Riquelme & Spitkovsky 2010)

$$\Gamma_B = 2\frac{J_{CR}}{c}\sqrt{\frac{\pi}{\rho}}\frac{v_A/c_s}{1+v_A/c_s} = \frac{\omega_{pi}n_{CR}v_s}{n_i c}\frac{v_A/c_s}{1+v_A/c_s}. \tag{23}$$

The resulting electron temperature may be estimated as follows. The electron velocity will be

$$v_e \simeq \frac{\Omega_{LH}}{k_\parallel} \simeq \frac{\Omega_e}{k} \tag{24}$$

since lower hybrid waves propagate within a cosine $\sqrt{\frac{m_e}{m_i}}$ of the perpendicular to the magnetic field. If we put $k \simeq 0.39\Omega_{LH}\left\langle\gamma\right\rangle n_i/n_{CR}v_d$ the electron kinetic energy is

$$\frac{1}{2}m_e v_e^2 \simeq \frac{m_i v_d^2}{2\times 0.39^2}\frac{n_{CR}^2}{n_i^2\left\langle\gamma\right\rangle^2} \simeq 8\times 10^8\frac{n_{CR}^2}{n_i^2\left\langle\gamma\right\rangle^2} \tag{25}$$

where we have put $v_d \simeq c/2$. For $n_{CR}/n_i\left\langle\gamma\right\rangle \sim 10^{-3}$, this gives electron energies of order 100 - 1000 eV, constant with shock velocity if this ratio is also constant. Requiring $\Omega_{LH}/v_e < k < \Omega_{LH}/v_i$ for lower hybrid waves yields the following inequality

$$\frac{0.78v_i}{c} < \frac{n_{CR}}{n_i\left\langle\gamma\right\rangle} < \frac{0.78v_e}{c} \tag{26}$$

which at $T = 10^4$K gives $2\times 10^{-5} < n_{CR}/n_i\left\langle\gamma\right\rangle < 10^{-3}$, consistent with the forgoing.

An analytic expression for the lower hybrid wave growth rate can be derived by dropping the last two terms in equation 22, which are of order $m_e/m_i$ relative to the other through their dependence on $\Omega_{CR}$, and solving the resulting cubic equation

$$\omega^3 - \omega\Omega_{LH}^2 + \mathbf{k}\cdot\mathbf{v}_d\frac{n_{CR}}{\left\langle\gamma\right\rangle n_i}\Omega_{LH}^2 = 0. \tag{27}$$

Using standard procedures (Abramowitz & Stegun 1984), the condition for complex roots becomes $\mathbf{k}\cdot\mathbf{v}_d n_{CR}/\left\langle\gamma\right\rangle n_i > \left(2/3\sqrt{3}\right)\Omega_{LH} = 0.385\Omega_{LH}$, in good agreement with the numerical solution above, and with predicted growth rate $\Gamma_{LH} = 2^{-1/3}3^{-1/2}A^{-2/3}\sqrt{A^2/4 - 1/27}\Omega_{LH}$ where $A = \mathbf{k}\cdot\mathbf{v}_d n_{CR}/\left\langle\gamma\right\rangle n_i\Omega_{LH}$.

In Fig. 2 we plot $\Gamma_{LH}$ against $\log_{10}A$ as a solid line. It increases monatonically from 0 at $A = 0.385$, ($\log_{10}A = -0.415$). We compare with $\Gamma_B$ plotted as dashed lines for

values of $c_s/v_A = 1$, 0.3, 0.1, and 0.03 (from equation 22, in units of $\Omega_{LH}\langle\gamma\rangle$). As the magnetic field becomes stronger, the lower hybrid wave growth rate becomes stronger relative to the growth rate for magnetic field amplification. At sufficiently large $A$, magnetic field amplification always wins, but there is always a range of lower $A$ where lower hybrid wave growth dominates. These dashed curves take a realistic electron-proton mass ratio. Riquelme & Spitkovsky (2010) present simulations with $m_e/m_i = 0.1$, and for this reason we give as dotted curves $\Gamma_B$ for the reduced mass ratio and the same values of $c_s/v_A$. The magnetic field amplification is much stronger in such circumstances, and the "window" in $A$ where lower hybrid wave growth dominates is much reduced, consistent with Riquelme & Spitkovsky (2010) who do not report any evidence of electron heating in their simulations. Riquelme & Spitkovsky (2011) also report a mass ratio dependence in their treatment of electron injection by whistlers. A detailed assessment of the electron heating at saturation will require a dielectric tensor accounting for electron thermal motions in place of equation 21, which will be deferred to a separate paper. However our simple treatment illustrates that in realistic conditions, lower hybrid wave growth may compete with magnetic field amplification and provide extra electron heating at fast efficient cosmic ray accelerating shocks.

## 4. The Forward Shocks of SN 1006, Cas A, and SNR 0509-67.5

### 4.1. Preamble

We have argued that electron heating at SNR shocks should break from the behavior discovered in shocks with $v_s < 3000\,\mathrm{km\,s^{-1}}$ by Ghavamian et al. (2007a) and van Adelsberg et al. (2008) at sufficiently high shock velocity where nonresonant magnetic field amplification sets in. Higher electron temperatures should be expected in this regime, because the shock precursor over which electron heating becomes longer than in the purely resonant case, or because magnetized cosmic rays may also contribute to electron heating through the drift instability treated in subsection 3.3. As a first step we therefore investigate the electron heating behind the forward shocks of SN 1006 and Cas A, which are faster than those studied in the samples above.

### 4.2. SN 1006

The likely remnant of a Type Ia supernova, SN 1006 is located 500 pc above the galactic plane, expanding into unusually low density interstellar medium. Having sustained high

shock speeds over a long period of time, it is the most effective accelerator of cosmic rays of all known SNRs.

SN 1006 was the first SNR from which the X-ray emission was conclusively identified as synchrotron radiation (Koyama et al. 1995, Reynolds 1996). This emission is strong on the NE and SW limbs. It has been demonstrated that the NE and SW synchrotron limbs represent "polar caps" (Willingale et al. 1996; Rothenflug et al. 2004; Reynoso et al. 2013), suggesting that particle acceleration (at least of electrons) is favored in this particular direction, which coincides with the likely direction of the galactic magnetic field (Leckband et al. 1989). Thus we should tentatively conclude that particle acceleration at quasi-parallel shocks (magnetic field aligned along shock velocity vector) is more favored than at quasi-perpendicular. Cassam-Chenaï et al. (2008) find the contact discontinuity closer to the forward shock in these regions (NE and SW) than elsewhere in the remnant, though Miceli et al. (2009) reach different conclusions. Rakowski et al. (2011) study knots of emission apparently ahead of the blast wave in the SE region. While the regular spacing between the three knots is consistent with what one would expect from the nonlinear saturation of the Bell instability, the spectra of these knots indicate that they are most likely ejecta. However in plasma with an adiabatic index of 5/3, such knots are not expected to move anywhere close to the blast wave, let alone overtake it. Rakowski et al. (2011) suggested, following Jun et al. (1996), that density perturbations ahead of the shock advected downstream induce extra vorticity that allows such knots to move ahead of the forward shock. In the case of SN 1006, situated high above the galactic plane, perturbations induced by a cosmic ray precursor are a plausible origin of such density structures.

A HESS detection of SN 1006 has been reported (Acero et al. 2010), consistent with an ambient gas density of 0.05 $\mathrm{cm}^{-3}$ (Acero et al. 2007). Proper motions have been measured in the optical, 0.28" $\mathrm{yr}^{-1}$ (in the NW, see Fig. 1; Winkler et al. 2003), corresponding to a shock velocity of $v_s = 2900$ km $\mathrm{s}^{-1}$ (assuming a distance of 2.2 kpc), and in X-rays at 0.48" $\mathrm{yr}^{-1}$ in the NE (Katsuda et al. 2009) giving 5000 km $\mathrm{s}^{-1}$, and at 0.3" - 0.49" in the NW (Katsuda et al. 2013) indicating higher density in the NW than elsewhere. Hamilton et al. (2007) derive a reverse shock velocity of 2700 km $\mathrm{s}^{-1}$, and determine the expansion velocity of ejecta entering the reverse shock to be 7000 km $\mathrm{s}^{-1}$ from HST observations. The NW limb is believed to have encountered higher densities, ($\sim 0.4$ $\mathrm{cm}^{-3}$), including partially neutral material giving rise to optical and UV spectra.

We model SN 1006 as expanding into a uniform density interstellar medium with density 0.05 amu $\mathrm{cm}^{-3}$, explosion energy $1 \times 10^{51}$ ergs, and ejecta mass 1.4 $M_\odot$, yielding a blast wave velocity of 4700 km $\mathrm{s}^{-1}$ and radius 8 pc at a distance of 2.2 kpc (Ghavamian et al. 2002). Figure 3 shows similar loci of electron temperature and ionization age behind the forward

shock for the cases of no preshock electron heating, and heating to $1 \times 10^6$, $3 \times 10^6$, and $1 \times 10^7$ K respectively moving upwards. We show data points for the SE synchrotron dim region given by Miceli et al. (2012, including their 95% confidence limits). These indicate a temperature of $5 \times 10^6 - 1 \times 10^7$ K in the precursor. This is significantly higher than the electron heating of $3 \times 10^6$ K determined at the NW limb by Ghavamian et al. (2007a), supporting our hypothesis. Note the this is an electron temperature immediately postshock, including any heating by adiabatic compression occurring upon shock passage, and so implies a temperature of $\sim 1 \times 10^6$ K in the precursor.

Assuming otherwise similar cosmic ray acceleration properties at the NW and SW limbs of SN 1006, the presence of neutrals in the NW, presumably indicative of a region of increased density in the interstellar medium which decelerates the shock, that must be making the difference. In our view, the shock has been decelerated in the NW to velocities where resonant magnetic field amplification dominates, whereas in the SE, nonresonant amplification is still operating, giving rise to the increased electron heating. The direct damping of Alfvén waves by charge exchange reactions is probably insignificant compared to other mechanisms of damping.

### 4.3. Cas A

Cas A offers a complementary case to SN 1006. It is a core collapse supernova remnant, which is expanding into dense remnant stellar wind. Since this ambient medium was presumably photoionized by the radiation from the supernova itself, neutrals are absent from the preshock gas. The preshock magnetic field could well be considerably different to the "canonical" interstellar medium values of $\sim 3\mu$G. The expansion of the stellar wind from the stellar atmosphere to the position where it is now encountered by the forward shock of the supernova remnant dilutes any pre-existing magnetic field to negligible strength. Any preshock magnetic field must be generated by motions within the stellar wind itself. The equipartition field for a wind moving at 20 km s$^{-1}$ would be 10 $\mu$G, taking a density of 2 amu cm$^{-3}$ from Hwang & Laming (2012). These parameters correspond to a mass loss rate of $10^{-4}$ M$_\odot$yr$^{-1}$. A lower mass loss rate, or the absence of means for the magnetic field to reach equipartition would imply a (much) lower preshock magnetic field.

To search for and obtain measured temperatures at the forward shock, we examined thirteen regions at and interior to the outermost filaments of Cas A, as shown in Figure 4. This search is complicated by two factors: the filaments are mostly dominated by synchrotron emission (Gotthelf et al. 2001; Helder & Vink 2008), and the faint outer regions of the remnant are strongly contaminated by scattering of emission from the bright ejecta ring.

As a dust scattering model is beyond the scope of our work, we chose a conservative approach in subtracting this scattered emission to identify secure examples of thermal X-ray emission associated with the forward shock. We select a local background region in the vicinity of each filament of interest, and model the spectrum in that region including a component for the particle background. The astrophysical component of the background spectrum is generally well-described by a thermal plane parallel shock model (*vpshock* in XSPEC) with variable abundances characteristic of the ejecta, and fitted temperatures and ionization ages similar to those obtained for ejecta regions by Hwang & Laming (2012). This background model is then frozen and included in the spectral model for the source region of interest, with only its overall normalization freely fitted. This is a simple and conservative way to remove the effect of the scattered emission from the bright ejecta ring as this scattered emission will vary depending on the relative positions of the source and background region (it is also energy-dependent). In most cases, the background region is outside the source region, and the fitted normalization is numerically larger, though of comparable scale, to the ratio of geometrical areas on the detector. This is at least consistent with the idea that scattered intensity is higher closer to the ejecta ring, but we found that the scale factor was always fitted higher than the geometrical scale factor, regardless of the relative position of source and background. Thus the thermal background emission is more likely to be oversubtracted than undersubtracted in our approach, and our identification of thermal emission associated with the forward shock should be conservative.

The source spectrum itself is fitted with a variety of model, including a pure power law and vpshock models with either ejecta-type element abundances or abundances characteristic of Cas A's expected circumstellar environment. We also considered models combining a power law with a forward shock type model. Regions were rejected for the purpose of this study if they were better fitted with ejecta-type abundances, or a power law or if the best-fitting thermal model for the forward shock had ionization age consistent with zero within its 90% confidence errors. The actual fitted ionization ages cannot be taken too seriously, as the spectral models are not likely to be very accurate at these very low ionization ages. The most that can be gleaned is that the thermal emission is present and that that ionization age is low. Possibly some of the rejected regions could actually contain detectable emission from the forward shock, but this could not be confidently determined without a sophisticated and careful treatment of the scattered background. Having been chosen conservatively, the two regions that remain are likely to represent instances of thermal emission associated with the forward shock. The best fitting of the models that we examined for these two regions were a combined power law and thermal forward shock model. Their fitted temperatures and ionization ages are given in Table 1, with 90% confidence limits.

We model Cas A very similarly to the preferred model for Cas A in Hwang & Laming

(2012); 3 $M_\odot$ ejecta, $2.4 \times 10^{51}$ ergs explosion energy, a product of blast wave radius and circumstellar density $\rho r_f^2 = 16$ amu pc$^2$, and the radius of a circumstellar bubble $R_{bub} = 0.3$ pc. The blast wave has velocity 5000 km s$^{-1}$ (at the current epoch) and is at a radius of 2.6 pc. The preshock medium is taken to be 49% H, 49% He, and 2% N by mass, reflecting the enrichment of the outer stellar layers in N by the CNO process. Relative to H, He and N are enhanced over solar values by factors of approximately 2 and 20 respectively.

Figure 5 shows the locus of electron temperature and ionization age (the product of electron density and time, $n_e t$) behind the forward shock for different values of electron heating in the precursor. From the lowest to the highest, they represent no heating, and heating to temperatures of $1 \times 10^6$, $3 \times 10^6$, $1 \times 10^7$ and $3 \times 10^7$ K respectively. Electrons are further heated by adiabatic compression on passage through the shock. The two points labeled "a" and "b" come from fits in Vink & Laming (2003), one from a synchrotron bright portion of the blast wave with higher electron temperature, and one from a synchrotron dim region with lower electron temperature. Also shown on Fig. 5 are points from fits to regions labeled "s4" and "sw", with locations within Cas A shown in Fig. 4. These both have lower $n_e t$ than regions "a" and "b", and so have undergone passage through the forward shock more recently. They also broadly support the inference from the other two, that of a precursor electron temperature in the range $1 \times 10^7 = 3 \times 10^7$ K, again significantly higher than the corresponding value from an extrapolation of the survey of Ghavamian et al. (2007a). Considering that the preshock magnetic field may be lower, possibly considerably lower, than that in SN 1006, the inference of postshock magnetic fields of order 100 $\mu$G (Vink & Laming 2003) suggests that nonnresonant magnetic field amplification and saturation should be at work, if cosmic rays are responsible. Unfortunately, it does not appear possible to detect such a precursor observationally, because of scattered light from the bright remnant interior. We also note that the circumstellar medium of Cas A, unlike that presumed for SN 1006, is naturally clumpy, and that in such circumstances, magnetic field amplification by the interaction of the shock with such pre-existing turbulence (Giacalone & Jokipii 2007), or variations upon this mechanism, (e.g. Beresnyak et al. 2009; Drury & Downes 2012) cannot so easily be ruled out.

### 4.4. SNR 0509-67.5

In our focus on higher shock velocities than those considered by Ghavamian et al. (2007a), results derived from SN 1006 and Cas A, while supportive of our hypothesis, are limited by the fact that the emission we observe comes from a region downstream of the shock itself, and electron heating at the shock front is derived by model extrapolation. This

is presumably because the H$\alpha$ emission studied by Ghavamian et al. (2007a) is strongest in regions where the shock encounters denser regions of interstellar medium; sufficiently dense that neutrals can survive against ionization, and the shock naturally decelerates in such regions. One possible example of a faster shock displaying H$\alpha$ emission is SNR 0509-67.5 (Helder et al. 2010). The remnant has forward shock velocities in the range 5200 - 6300 km s$^{-1}$ (Ghavamian et al. 2007b), derived from the width of the Ly$\beta$ line.

The H$\alpha$ line profile consists of two components; a narrow feature arising as preshock neutrals diffuse through the shock and are excited before being ionized by shocked ions and electrons, and a broad component with an origin in charge exchange, as a preshock neutral has its electron captured by a shocked proton. The intensity ratio between these two can be a diagnostic of the electron temperature. If the neutrals are primarily destroyed by electron impacts, then the broad/narrow intensity ratio will be small (i.e. not enough slow neutrals survive long enough to become fast neutrals by charge exchange), but if the electrons are inefficient at ionizing neutrals, because of insignificant electron heating at the shock, the broad component becomes comparable in intensity to the narrow feature.

In SNR 0509-67.5, the broad component intensity is significantly smaller than that of the narrow component, indicating the presence of electron heating. The analysis of Helder et al. (2010) also accounts for shock energy losses to cosmic rays, corroborating the shock speeds derived by Ghavamian et al. (2007b), and finding electron/proton temperature ratios in the range 0.2 - 1, significantly larger than those found by Ghavamian et al. (2007a). While more uncertain than the SN 1006 or Cas A results given above, the elevated electron temperature is determined at the forward shock itself, and further supports the argument of this paper.

## 5. Conclusions

In this paper we have attempted to hypothesize how electron heating at collisionless shocks might behave in the absence of neutrals in the preshock medium, and in the presence of magnetic field amplification by the nonresonant cosmic ray current driven instability. Compared to shocks dominated by resonant magnetic field amplification where the precursor length $L \simeq \varkappa/v_s$, shocks with magnetic field amplified by the nonresonant instability have $L$ decreasing less quickly with increasing $v_s$. The time spent in the precursor, $t = L/v_s$ decreases more slowly than $1/v_s^2$, leading to an increase in the electron temperature expected if the electron heating is mediated by cosmic ray generated lower hybrid waves with velocity diffusion coefficient proportional to $v_s^2$. Thus at shocks of higher velocities than those in the samples of Ghavamian et al. (2007a) and van Adelsberg et al. (2008), we speculate that the electron temperature should rise with increasing shock speed. Analysis of the

electron temperature behind higher speed shocks in Cas A and in SN 1006 supports this view, within observational uncertainties, as do observations of Balmer emission from SNR 0509-67.5 (Helder et al. 2010).

At still higher shock speeds, a drift instability due to magnetized cosmic rays may also begin to heat electrons. The threshold speed where this might begin is uncertain, but of order 10,000 km $s^{-1}$. Observations of higher velocity shocks are obviously very interesting in this regard. Of accessible supernova remnants, 1E0102 and SN 1987A would seem to be the prime candidates. Hughes et al. (2000) infer a forward shock velocity for 1E0102 from proper motion measurements of 6000 km $s^{-1}$. This forward shock, however, is running into a remnant stellar wind, which may itself have a speed of 2000 - 3000 km $s^{-1}$, thus reducing the actual forward shock velocity with respect to the upstream medium. Further, Flanagan et al. (2004) only infer expansion velocities of order 1000 km $s^{-1}$ from observations of the SNR ejecta. The forward shock of SN 1987A is currently running into the inner circumstellar ring (Zhekov et al. 2005). The fast deceleration means that the shock velocity is uncertain, and the spectrum obtained necessarily has contributions from decelerated and relatively undecelerated portions of the blast wave, making precise interpretation difficult. A further complication here is that SN 1987A is relatively young, and it is unclear how much energy has yet accumulated in cosmic rays at its forward shock.

This work was supported by the NASA ADP program (UH, JML and CER), and by basic research funds of the Office of Naval Research (JML and CER). JML would also like to acknowledge the hospitality of R. Bingham during a visit to the Rutherford Appleton Laboratory, where some of this work was started.

## A. Cosmic Ray Distributions

The cosmic ray distribution is taken to be

$$f_{CR}\left(p\right) = \frac{n_{CR} p_0^{1+a} p_{max}^{1+a}}{4\pi \left(p_{max}^{1+a} - p_0^{1+a}\right) p^{4+a}} \tag{A1}$$

where $p_0$ and $p_{max}$ are the lower and upper limits on the cosmic ray momentum respectively. The cosmic ray kinetic energy is

$$\begin{aligned} E_{CR} &\simeq \int_{p_0}^{mc} f_{CR} \frac{p^2}{2m} 4\pi p^2 dp + \int_{mc}^{p_{max}} f_{CR} \left(pc - mc^2\right) 4\pi p^2 dp \\ &\simeq n_{CR} \frac{p_0^2}{2m} \left[\frac{1 - \left(mc/p_0\right)^{1-a}}{a-1}\right] + n_{CR} p_0 c \left(\frac{p_0}{mc}\right)^a \left[\frac{1 - \gamma_{max}^{-a}}{a}\right] \end{aligned} \tag{A2}$$

where $\gamma_{max} = p_{max}/mc$ and $p_{max} >> p_0$. When $a = 1$ or $a = 0$ in the first or second terms respectively, the quantities in square brackets become $\ln(mc/p_0) - 1$ and $\ln\gamma_{max} - 1$ respectively. The relativistic contribution dominates, except where $a >> 1$ and $mc >> p_0$. Given that $a = 0$ reproduces the standard cosmic ray spectrum resulting from first order Fermi acceleration at a strong shock, and the $p_0 \sim mc$ is frequently required for injection, we neglect the nonrelativistic contribution in the following. Specializing to $a = 0$ for the time being we also write the cosmic ray number density $n_{CR}$ in terms of the ratio of cosmic ray pressure to shock ram pressure $\eta = P_{CR}/\rho v_s^2$ as follows

$$n_{CR} = \frac{E_{CR}}{p_0 c\left(\ln\gamma_{max} - 1\right)} = \frac{3\eta\rho v_s^2}{p_0 c\left(\ln\gamma_{max} - 1\right)}. \tag{A3}$$

With $\rho = n_i m$ and $p_0 = m v_{inj}$ this simplifies to

$$\frac{n_{CR}}{n_i} = \frac{3\eta v_s^2}{c v_{inj}\left(\ln\gamma_{max} - 1\right)} \simeq \frac{3\eta v_s^2}{c^2\left(\ln\gamma_{max} - 1\right)}. \tag{A4}$$

The average cosmic ray kinetic energy

$$\langle E_{CR}\rangle = \frac{E_{CR}}{n_{CR}} = p_0 c\left(\ln\gamma_{max} - 1\right) = \left(\langle\gamma\rangle - 1\right) mc^2 \tag{A5}$$

so $\langle\gamma\rangle \simeq \left(\ln\gamma_{max} - 1\right) \times v_{inj}/c + 1 \simeq \ln\gamma_{max}$ if $v_{inj} \simeq c$.

Considering a subpopulation of unmagnetized cosmic rays with $p > p_1$, their density $n'_{CR}$ is given by

$$n'_{CR} = \int_{p_1}^{p_{max}} f_{CR} 4\pi p^2 dp = n_{CR}\left(\gamma_{max} - \gamma_1\right)/\gamma_{max}\gamma_1, \tag{A6}$$

and the average unmagnetized cosmic ray kinetic energy, $E'_{CR}$ by

$$E'_{CR} = \int_{p_1}^{p_{max}} f_{CR}\left(pc - mc^2\right) 4\pi p^2 dp = n_{CR} mc^2\left(\ln\gamma_{max} - \ln\gamma_1 + 1/\gamma_{max} - 1/\gamma_1\right). \tag{A7}$$

These lead to the average Lorentz factor for the unmagnetized cosmic rays of

$$\langle\gamma'\rangle = \frac{\gamma_1\gamma_{max}}{\gamma_{max} - \gamma_1} \ln\frac{\gamma_{max}}{\gamma_1}. \tag{A8}$$

For $a \neq 0$, we give the following more general results,

$$\frac{n_{CR}}{n_i} = \frac{3\eta v_s^2}{c^2}\left(\frac{c}{v_{inj}}\right)^a \frac{a}{1 - \gamma_{max}^{-a}} \tag{A9}$$

$$\langle\gamma\rangle = 1 + \left(\frac{v_{inj}}{c}\right)^{1+a} \left[\frac{1-\gamma_{max}^{-a}}{a}\right] \tag{A10}$$

$$n'_{CR} = \frac{n_{CR}}{1+a} \frac{\gamma_{max}^{1+a} - \gamma_1^{1+a}}{\gamma_{max}^{1+a}\gamma_1^{1+a}} \left(\frac{v_{inj}}{c}\right)^{1+a} \tag{A11}$$

$$\langle\gamma'\rangle = \left(\frac{v_{inj}}{c}\right)^{1+a} \frac{\gamma_{max}\gamma_1}{a} \frac{\gamma_{max}^a - \gamma_1^a}{\gamma_{max}^{1+a} - \gamma_1^{1+a}}. \tag{A12}$$

$$\tag{A13}$$

## REFERENCES


Abramowitz, M., & Stegun, I. A. 1984, Handbook of Mathematical Functions, (Verlag Harri Deutsch: Frankfurt am Main)

Acero, F., Ballet, J. & Decourchelle, A. 2007, A&A, 475, 883

Acero, F., Aharonian, F., Akhperjanian, A. G., et al. 2010, A&A, 516, A62

Bamert, K., Kallenbach, R., Ness, N. F., et al. 2004, ApJ, 601, L99

Bell, A. R., & Lucek, S. G. 2001, MNRAS, 321, 433

Bell, A. R. 2004, MNRAS, 353, 550

Bell, A. R. 2005, MNRAS, 358, 181

Bell, A. R., Schure, K. M., Reville, B., & Giacinti, G. 2013, MNRAS, 431, 415

Beresnyak, A., Jones, T. W., & Lazarian, A. 2009, ApJ, 707, 1541

Caprioli, D., & Spitkovsky, A. 2013, ApJ, 765, L20

Cargill, P. J., & Papadopoulos, K. 1988, ApJ, 329, L29

Cassam-Chenaï, G., Hughes, J. P., Ballet, J., & Decourchelle, A. 2007, ApJ, 665, 315

Cassam-Chenaï, G., Hughes, J. P., Reynoso, E. M., Badenes, C. & Moffett, D. 2008, ApJ, 680, 1180

Drury, L. O'C., & Downes, T. P. 2012, MNRAS, 427, 2308

Flanagan, K. A., Canizares, C. R., Dewey, D., Houck, J. C., Fredericks, A. C., Schattenburg, M. L., Markert, T. H., & Davis, D. S. 2004, ApJ, 605, 230

Gargaté, L., Fonseca, R. A., Niemiec, J., Pohl, M., Bingham, R., & Silva, L. O. 2010, ApJ, 711, L127

Gargaté, L., & Spitkovsky, A. 2012, ApJ, 744, 67

Ghavamian, P., Winkler, P. F., Raymond, J. C., & Long, K. S. 2002, ApJ, 572, 888

Ghavamian, P., Laming, J. M., & Rakowski, C. E. 2007, ApJ, 654, L69

Ghavamian, P., Blair, W. P., Sankrit, R., Raymond, J. C., & Hughes, J. P. 2007, ApJ, 664, 304

Ghavamian, P., Schwartz, S. J., Mitchell, J., Masters, A., & Laming, J. M. 2013, Space Science Reviews, 178, 633

Giacalone, J., & Jokipii, J. R. 2007, ApJ, 663, L41

Gotthelf, E. V., Koralesky, B., Rudnick, L., Jones, T. W., Hwang, U., & Petre, R. 2001 ApJ, 552, L39

Hamilton, A. J. S., Fesen, R. A., & Blair, W. P. 2007, MNRAS, 381, 771

Helder, E. A., Kosenko, D. & Vink, J. 2010, ApJ, 719, L140

Helder, E. A., & Vink, J. 2008, ApJ, 686, 1094

Hughes, J. P., Rakowski, C. E., & Decourchelle, A. 2000, ApJ, 543, L61

Jun, B.-I., Jones, T. W., & Norman, M. L. 1996, ApJ, 468, L59

Hwang, U., & Laming, J. M. 2012, ApJ, 746, 130

Katsuda, S., Petre, R., Long, K. S., Reynolds, S. P., Winkler, P. F., Mori, K., & Tsunemi, H. 2009,ApJ, 692, L105

Katsuda, S., Long, K. S., Petre, R., Reynolds, S. P., Williams, B. J., & Winkler, P. F. 2013, ApJ, 763, 85

Koyama, K., Petre, R., Gotthelf, E. V., Hwang, U., Matsuura, M., Ozaki, M., & Holt, S. S. 1995, Nature, 378, 255

Laming, J. M. 2001a, ApJ, 546, 1149

Laming, J. M. 2001b, ApJ, 563, 828

Laming, J. M., Moses J. D., Ko, Y.-K., Murphy, R. J., Ng, C. K., Rakowski, C. E., & Tylka, A. J. 2013, ApJ, 770, 73

Leckband, J. A., Spangler, S. R., & Cairns, I. H. 1989, ApJ, 338, 963

Long, K. S., Reynolds, S. P., Raymond, J. C., Winkler, P. F., Dyer, K. K., & Petre, P. 2003, ApJ, 586, 1162

Lucek, S. G., & Bell, A. R. 2000, MNRAS, 314, 65

Luo, Q., & Melrose, D. 2009, MNRAS, 397, 1402

Marcowith, A., & Casse, F. 2010, A&A, 515, 90

Matsukiyo, S. 2010, Physics of Plasmas, 17, 042901

Miceli, M., Bocchino, F., Iakubovskyi, D., Orlando, S., Telezhinsky, I., Kirsch, M. G. F., Petruk, O., Dubner, G., & Castelletti, G. 2009, A&A, 501, 239

Miceli, M., Bocchino, F., Decourchelle, A., Maurin, G., Vink, J., Orlando, S., Reale, F., & Broersen, S. 2012, A&A, 546, A66

Morlino, G., Amato, E., Blasi, P., & Caprioli, D. 2010, MNRAS, 405, L21

Nekrasov, A. K., & Shadmehri, M. 2012, ApJ, 756, 77

Niemiec, J., Pohl, M., Bret, A., & Stroman, T. 2010, ApJ, 709, 1148

Rakowski, C. E., Laming, J. M., & Ghavamian, P. 2008, ApJ, 684, 348

Rakowski, C. E., Ghavamian, P., & Laming, J. M. 2009, ApJ, 696, 2195

Rakowski, C. E., Laming, J. M., Hwang, U., Eriksen, K. A., Ghavamian, P., & Hughes, J. P. 2011, ApJ, 735, L21

Reville, B., & Bell, A. R. 2013, MNRAS, 430, 2873

Reynolds, S. P. 1996, ApJ, 459, L13

Reynoso, E. M., Hughes, J. P., & Moffett, D. A. 2013, AJ, 145, 104

Riquelme, M. A., & Spitkovsky, A. 2009, ApJ, 694, 626

Riquelme, M. A., & Spitkovsky, A. 2010, ApJ, 717, 1054

Riquelme, M. A., & Spitkovsky, A. 2011, ApJ, 733, 63

Rothenflug, R., Ballet, J., Dubner, G., Giacani, E., Decourchelle, A., & Ferrando, P. 2004, A&A, 425, 121

Stroman, T., Pohl, M., & Niemiec, J. 2009, ApJ, 706, 38

Stroman, T., Pohl, M., Niemiec, J., & Bret, A. 2012, ApJ, 746, 24

van Adelsberg, M., Heng, K., McCray, R., & Raymond, J. C. 2008, ApJ, 689, 1089

Vink, J., & Laming, J. M. 2003, ApJ, 584, 758

Völk, H. J., Berezhko, E. G., & Ksenofontov, L. T. 2005, A&A, 433, 229

Warren, J. S., Hughes, J. P., Badenes, C., Ghavamian, P., McKee, C. F., Moffett, D., Plucinsky, P. P., Rakowski, C., Reynoso, E., & Slane, P. 2005, ApJ, 634, 376

Wiener, J., Zweibel, E. G., & Peng Oh, S. 2013, arXiv:1301.4445

Willingale, R., West, R. G., Pye, J. P., & Stewart, G. C. 1996, MNRAS, 278, 749

Winkler, P. F., Gupta, G., & Long, K. S. 2003, ApJ, 585, 324

Winkler, P. F., Williams, B. J., Reynolds, S. P., Petre, R., Long, K. S., Katsuda, S., & Hwang, U. 2014, ApJ, 781, 65

Winske, D., & Leroy, M. M. 1984, J. Geophys. Res., 89, 2673

Yamazaki, R., Yoshida, T., Terasawa, T., Bamba, A., & Koyama, K. 2004, A&A, 416, 595

Zank, G. P., Li, G., Florinski, V., Hu, Q., Lario, D., & Smith, C. W. 2006, J. Geophys. Res. Space Phys., 111, 6108

Zhekov, S. A., McCray, R., Borkowski, K. J., Burrows, D. N., & Park, S. 2005, ApJ, 628, L127

This preprint was prepared with the AAS LaTeX macros v5.2.

Table 1: Cas A Forward Shock Fit Results

| region | $kT$ (keV) | $n_e t$ ($\mathrm{cm^{-3}s^{-1}}$) | $\chi^2$/dof |
|---|---|---|---|
| sw | 2.6 [2.2 - 3.0] | 8.4e9 [7.4e9 - 9.3e9] | 1.48 |
| s4 | 2.6 [2.3 - 2.9] | 9.6e8 [7.4e8 - 1.3e9] | 1.21 |

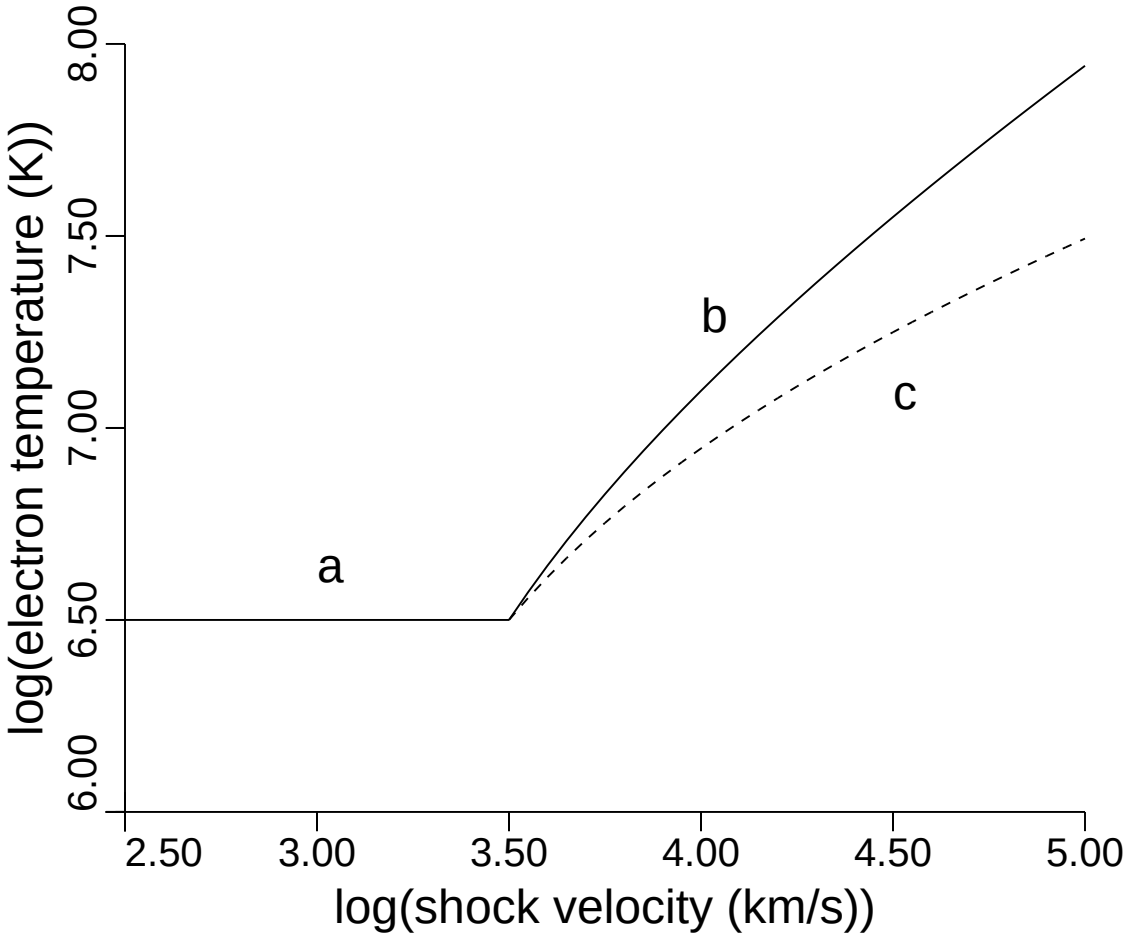


Fig. 1.— Schematic diagram showing the hypothesized variation of post shock electron temperature with shock velocity. At low shock speeds, the branch of the plot labeled "a" shows constant electron heating where cosmic rays resonantly amplify magnetic field. With constant cosmic ray diffusion coefficient $D$, the length of the precursor $L \sim \varkappa/v_s$, so the time spent in the precursor by preshock gas $t \sim \varkappa/v_s^2$, leading to electron heating $\sim D_{|||}t$ independent of $v_s$ where $D_{|||} \propto v_s^2$ is the diffusion coefficient in velocity space for electrons in lower hybrid waves. The branch labeled "c" shows the behavior when magnetic field in non-resonantly amplified, but resonantly saturated and $L \propto v_s^{-4/5} \ln v_s$, and branch "b" shows the completely nonresonant case, with $L \propto v_s^{-1/2} \ln v_s$. The break between resonant and nonresonant amplification at $v_s = 3000$ km s$^{-1}$ is motivated by the discussion in Marcowith & Casse (2010), but remains uncertain. Branch "c" is shown as a dashed line, because in this case the magnetic field amplification growth rate is always larger than that for lower hybrid waves.

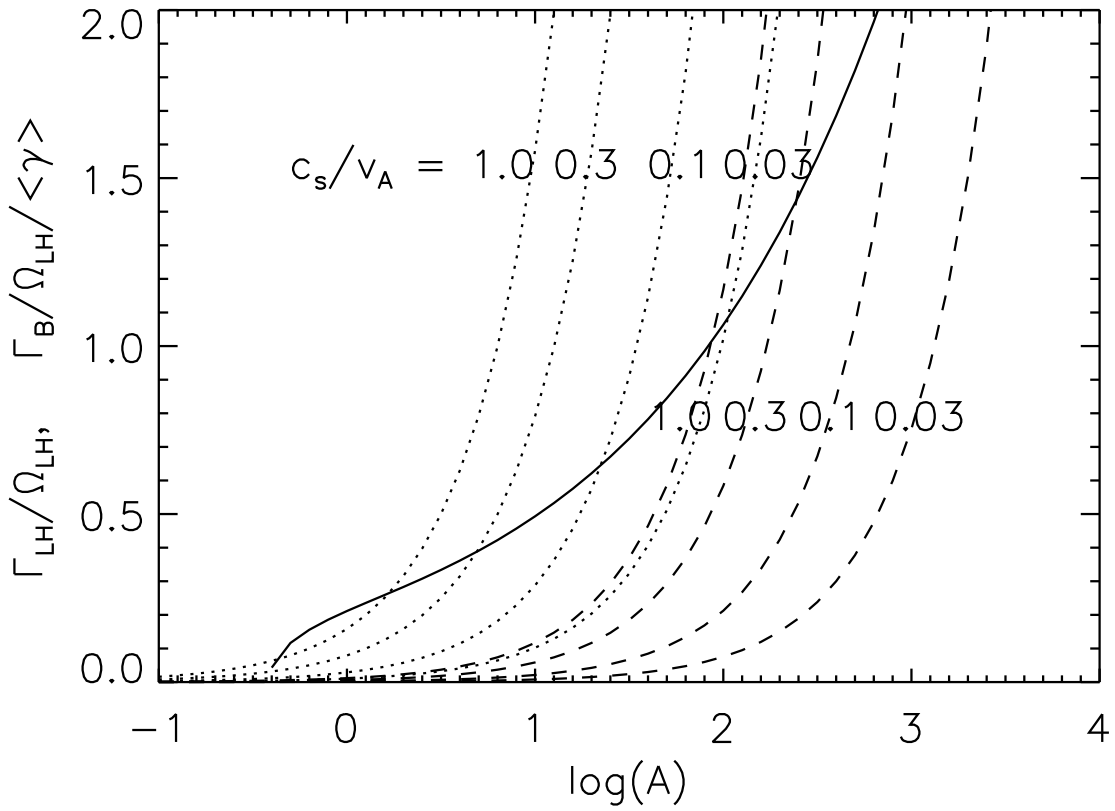


Fig. 2.— Growth rates for lower hybrid waves ($\Gamma_{LH}$) and magnetic field amplification ($\Gamma_B$), scaled by $\Omega_{LH}$, by magnetized cosmic rays in a shock precursor, against $\log_{10} A = \log_{10} (\mathbf{k} \cdot \mathbf{v}_d n_{CR} / \langle\gamma\rangle n_i \Omega_{LH})$. The solid curve gives $\Gamma_{LH}$. Dashed curves give values of $\Gamma_B$ for $c_s/v_A = 1$, 0.3, 0.1, 0.03 successively from the left, with higher growth for lower $c_s/v_A$. At sufficiently high $A$, $\Gamma_B$ is always dominant, but a region of lower $A$ exists where $\Gamma_{LH}$ is larger, and lower-hybrid wave growth may occur. The dotted curves give similar values for $\Gamma_B$, but using an electron-proton mass ratio of 10, to match this parameter in Riquelme & Spitkovsky (2010). Lower hybrid waves, and the ensuing electron heating, are much less favored in such conditions, because the magnetic field amplification is stronger.

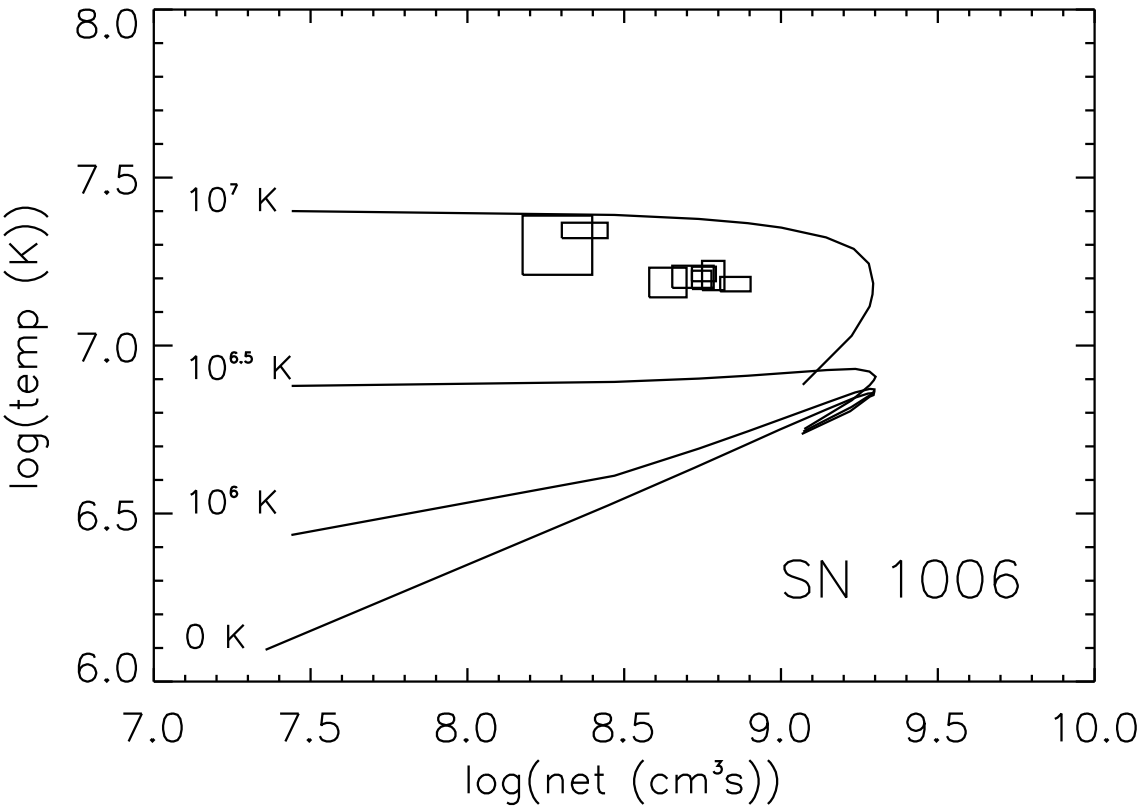


Fig. 3.— The locus of electron temperature $T_e$ against ionization age $n_e t$ for the forward shock of SN 1006, for four different degrees of electron-ion equilibration at the shock. The model is for a $1 \times 10^{51}$ erg explosion, $1.4 M_\odot$ ejecta, interstellar medium density of 0.05 cm$^{-3}$, and an ejecta envelope power law of 7. The lowest curve shows the case of no equilibration. The succeeding curves give models for electron heating in the shock precursor to temperatures of $1 \times 10^6$, $3 \times 10^6$ and $1 \times 10^7$ K. On passage through the shock these temperatures increase by a further factor of $4^{2/3}$ due to adiabatic compression. The boxes indicate data points from Miceli et al. (2012), with 95% confidence limits.

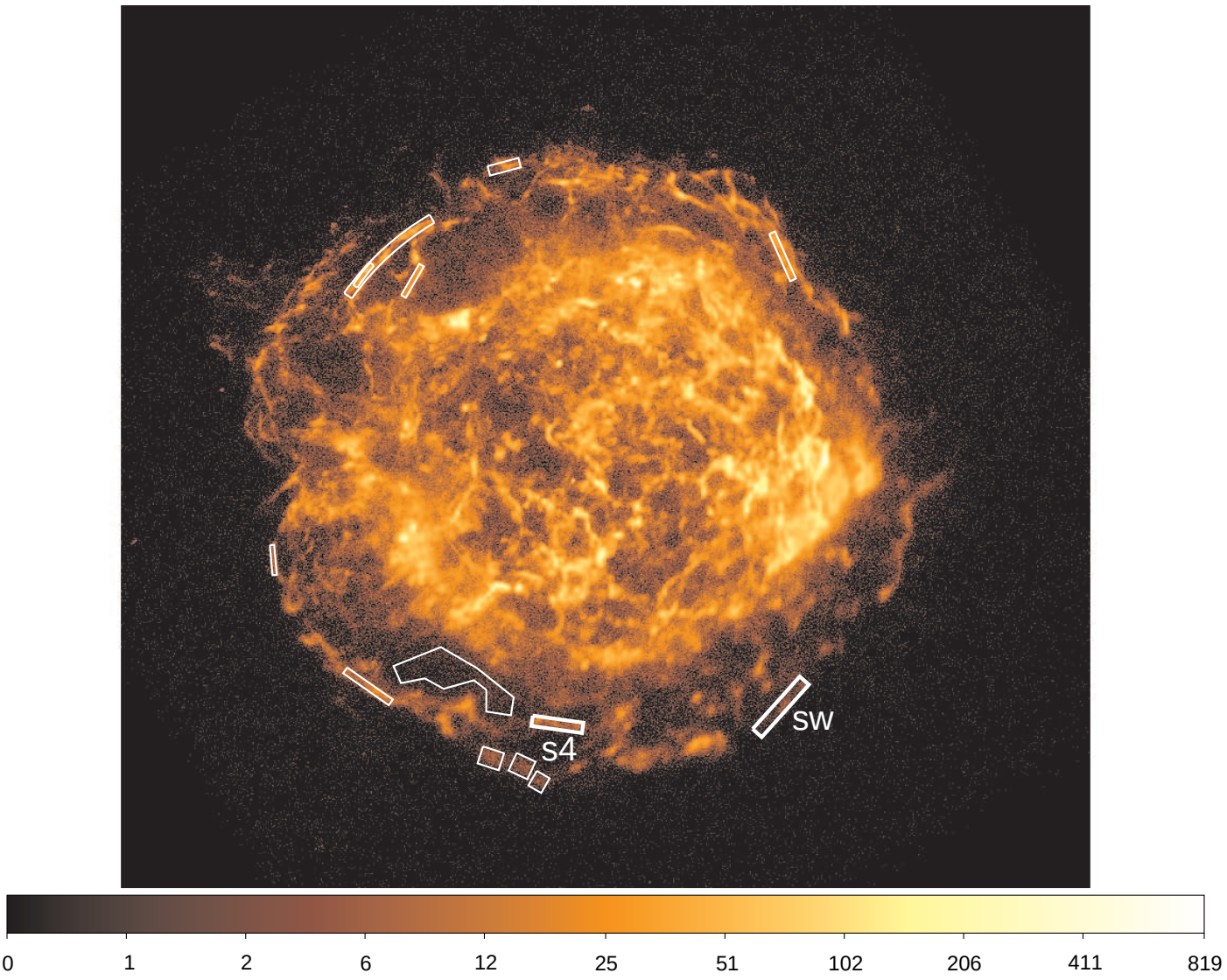


Fig. 4.— Positions of the thirteen regions in the Cas A SNR examined for this paper are shown superposed on a log intensity image of the 4-6 keV X-ray continuum of Cas A from Hwang et al. 2004, and this work. The "s4" and "sw" regions are labelled.

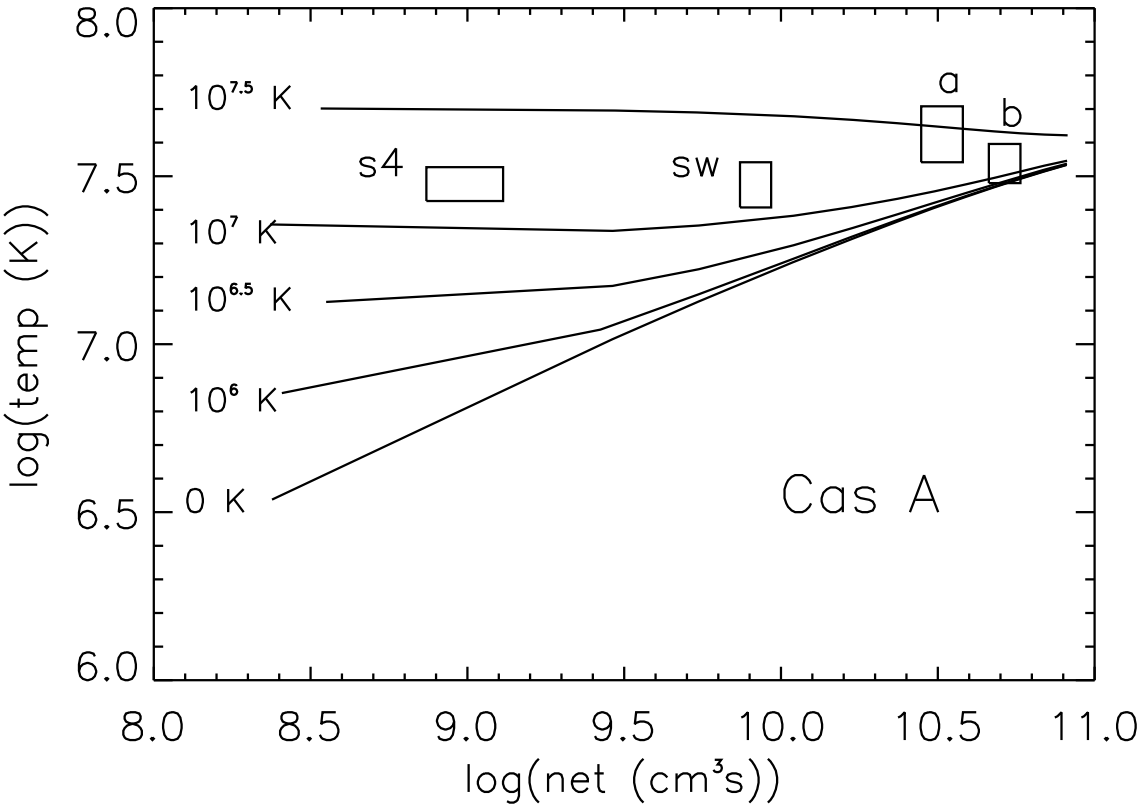


Fig. 5.— The locus of electron temperature $T_e$ against ionization age $n_e t$ for the forward shock of Cassiopeia A, for four different degrees of electron-ion equilibration at the shock. The lowest curve shows the case of no equilibration. The succeeding curves give models for electron heating in the shock precursor to temperatures of $1 \times 10^6$, $3 \times 10^6$, $1 \times 10^7$ and $3 \times 10^7$ K. On passage through the shock these temperatures increase by a further factor of $4^{2/3}$ due to adiabatic compression. The boxes indicate data points from Vink & Laming (2003); "a" comes from a bright X-ray synchrotron filament, while "b" comes from a dim synchrotron filament.